Phi: Jurnal Pendidikan Fisika dan Terapan
Vol. 13, No. 1 (2027) 15-30
ISSN: 2460-4348, e-ISSN: 2549-7162
https://jurnal.ar-raniry.ac.id/index.php/jurnalphi/index

Article Type: *original research*

Development of DEXS: A Simple GNU Octave-Based Software for Very Low Frequency Electromagnetic (VLF-EM) Data Processing

Dwi Santi Lestari[1], Anggie Susilawati[1], Muhamad Santri Nurinsani[1], Xena Wilhelmina Manalu[1], Muhammad Enzy Taura[1], Meylani Shintia Rachayu[1], Kensi Aryangga[1]
[1]Department of Geophysics, Faculty of Mathematics and Natural Sciences, Universitas Padjadjaran, Sumedang, West Java, Indonesia

Correspondence E-mail: anggie@geophys.unpad.ac.id

ARTICLE INFO

Article History:
Received: 10 May 2026
Revised: 31 July 2026
Accepted: 08 August 2026
Published: 09 August 2026

Keywords:
Very low frequency; Fraser filter; GNU octave; Karous–Hjelt filter; Pseudo-section; Software; VLF-EM

ABSTRACT

Very Low Frequency Electromagnetic (VLF-EM) data processing currently faces two major challenges: limited accessibility due to the high licensing costs of commercial software and the limited capabilities of existing software. This study aims to develop a simple software package, named DEXS, featuring a Graphical User Interface (GUI) on the GNU Octave platform as a freely accessible open-source alternative. DEXS was developed as a single .m script and designed to integrate the entire VLF-EM data processing workflow within a unified interface, including data import, averaging of repeated measurements at each station, application of the Fraser Filter and Karous–Hjelt Filter, and visualization of results in the form of graphs and two-dimensional pseudo-section maps. The software was evaluated using two VLF-EM field datasets by comparing the outputs generated by DEXS with those produced by KHFILT. The results show that the Fraser Filter graphs, Karous–Hjelt graphs, and pseudo-section maps generated by DEXS exhibit anomaly patterns that are consistent and comparable with those produced by KHFILT. Quantitative validation using cross plot analysis yielded a very strong linear relationship ($R^2 > 0.999$), confirming that the implemented algorithms are mathematically consistent and valid for qualitative subsurface structure interpretation. DEXS also provides more comprehensive capabilities than KHFILT, including support for six-column measurement parameter input, simultaneous visualization of two survey lines, and additional displays of out-phase and field strength data. These capabilities contribute to the development of open-source geophysical software by providing an integrated, validated, and freely accessible VLF-EM data processing system that supports both educational and research applications.

This work is licensed under a Creative Commons Attribution-ShareAlike 4.0 International License

1. INTRODUCTION

Geophysical methods are methods used to map the subsurface structure of the Earth by utilizing the principles of physics using measuring instruments (Purwanto et al., 2015). One commonly used method is the Very Low Frequency Electromagnetic (VLF-EM) method, which utilizes signal radiation from a radio transmitter at frequencies around 15–30 kHz (Desifatma et al., 2024; Hutchinson & Barta, 2002; Vargemezis et al., 2024). This method is based on measuring the Earth's response to planar electromagnetic waves generated by military navigation transmitters

located far from the survey area (Jeng et al., 2004; Paál, 1965; Saydam, 1981). The working principle of this method is based on inducing of a primary electromagnetic field that interacts with subsurface conductive materials, thereby generating a secondary electromagnetic field (Desifatma et al., 2024). In practice, the VLF-EM method is known to be effective and relatively economical for detecting various geological features such as fractures, weathering zones, aquifers, and sulfide mineralization (Alao et al., 2024; Al-Tarazi et al., 2008; Gürer et al., 2009; Telford et al., 1990).

Data obtained from field measurements are generally still in the form of raw data, which are typically recorded as in-phase and quadrature (out-phase) components (Widyaningrum et al., 2018). These data often show complex patterns, making them difficult to interpret geologically without further processing (Sundararajan et al., 2006). Therefore, data processing steps are required to highlight anomalies related to subsurface structures. Some commonly used processing techniques include the Fraser Filter, which converts intersection points into anomaly peaks (Fraser, 1969; Yadi et al., 2017), as well as the Karous–Hjelt Filter, which is used to estimate the distribution of equivalent current density with respect to depth and to generate two-dimensional subsurface cross-sectional visualizations (Karous & Hjelt, 1983; Monteiro Santos et al., 2006). Furthermore, data transformation and visualization processes are crucial for helping to identify the position and depth of anomalies more clearly, although estimating the depth of subsurface targets often poses a challenge of its own in VLF-EM surveys (Alao et al., 2024; Khalil & Santos, 2014). This is essential to support both qualitative and quantitative geological interpretation processes so that the picture of subsurface resistivity distribution becomes more accurate (Desifatma et al., 2024).

One of the challenges still faced in geophysical data processing is limited access to software capable of efficiently supporting all stages of data processing. Most geophysical software currently available is commercial and requires paid licenses at relatively high cost (Gordon & Santos, 2016), which can be a barrier for students and academics in learning and performing data processing independently. In addition to licensing issues, the available software is not yet fully capable of integrating data processing, visualization, and interpretation into a single workflow. Zlotnicki et al. (2006) emphasized that many standard visualization software packages are inadequate for effectively addressing data processing needs, so practitioners need to develop tools better suited to research requirements. Sundararajan et al. (2006) developed a MATLAB-based VLF data processing code known as VLFPROS to process VLF-EM data, which enables the creation of stacked profiles and contour maps to visualize the distribution of conductive materials beneath the surface. However, using this platform still requires a paid MATLAB software license (Sundararajan et al., 2006). On the other hand, the KHFILT software developed by Pirttijärvi (2004) has also been widely used to visualize the results of the Fraser Filter and the Karous–Hjelt Filter applied to VLF-EM data (Alao et al., 2024; Monteiro Santos et al., 2006). However, KHFILT has limitations in terms of processing capabilities, including the need to manually calculate the average of repeated measurements using external software, the fact that it only accepts input in the form of distance columns and in-phase values, its inability to display out-phase components or field strength, and its limitation to processing only one dataset per processing session. These conditions indicate that the need for software development is not only related to accessibility but also to the ability to integrate all stages of data processing into a single, user-friendly system.

GNU Octave is one platform that meets these needs because its syntax is very similar to MATLAB's and it supports numerical computation, matrix operations, data visualization, Graphical User Interface (GUI) development, and a variety of numerical libraries sufficient for implementing scientific algorithms without software licensing constraints (Purnama et al., 2025; Quarteroni et al., 2010). This study focuses on the design of a simple software tool called DEXS, developed using the GNU Octave platform. The DEXS software is designed as a simple and interactive GUI to integrate all stages of VLF-EM data processing from data loading, calculation of the average of repeated measurements, application of the Fraser Filter and Karous–Hjelt Filter, to visualization of results in the form of graphs and two-dimensional pseudo-sections, within a single integrated interface. This approach allows the entire data processing workflow to be carried out continuously without requiring additional software at each processing stage, making the processing more efficient, systematic, and easily reproducible. The validity of the developed software was evaluated by

comparing the processing results with those of the KHFILT software using both visual and quantitative analyses via linear regression (cross plot). The main contribution of this research lies not only in the development of open-source software but also in the provision of a VLF-EM data processing system that integrates all processing stages into a single interface with validated results. DEXS is expected to serve as a practical, easily accessible software alternative that supports learning and research activities in academic settings.

2. METHODS

2.1 Research Design

This research focuses on the development of software to design and implement a VLF-EM data processing application called DEXS using GNU Octave version 10.1.0. The development process includes software design, implementation of data processing algorithms, development of a GUI, and software validation. The implemented processing algorithms include calculating the average of repeated measurements for each station, applying the Fraser Filter, applying the Karous–Hjelt Filter, and visualizing the processing results in the form of graphs and two-dimensional pseudo-sections.

Software validation was performed by comparing the output generated by DEXS with that generated by the KHFILT software using the same field dataset. This comparison included both qualitative and quantitative evaluations. Qualitative validation was performed by comparing the Fraser Filter plots, Karous–Hjelt plots, and pseudo-section visualizations, while quantitative validation was performed using linear regression analysis (cross plots) to evaluate the numerical agreement between the outputs of the two software packages.

2.2 Research Data and Instruments

The data used in this study consist of VLF-EM measurement data stored in .dat file format. The data contain field measurement results from several observation points, organized into several columns of measurement parameters. The data structure in the input file consists of:
Column 1: Position or number of the measurement point (Station)
Column 2: Distance (m)
Column 3: In-phase value (%)
Column 4: Out-phase value (%)
Column 5: Field strength (μV/m)
Column 6: Transmitter frequency (kHz)

The VLF-EM measurement process in the field typically involves recording each measurement point three times to improve data reliability. Therefore, in the data files used in this study, a single station number may appear three times in a row, representing repeated measurements at the same location.

The instruments used in this study include a computer as the primary device for software development and testing. DEXS was developed and executed using GNU Octave version 10.1.0 on a laptop equipped with an Intel® Core™ i5-10310U CPU running at 1.70 GHz and 16 GB of RAM. This hardware configuration demonstrates that the proposed software can be developed and operated on a standard mid-range laptop without requiring high-performance computing resources. The data used consist of VLF-EM measurement data, which serve as test data in the development process and for evaluating the performance of the designed data processing software.

2.3 VLF Data Processing Workflow

The data processing steps in this study were carried out in stages, starting with data reading, calculating averages, filtering, and visualizing the results. The data processing stages began with reading .dat files containing VLF-EM measurement parameters from the field. After the data were loaded into the software, the first step was the averaging process. This process calculated the average value from three measurements at each station along a single measurement line. The purpose of this process is to reduce data variation caused by measurement fluctuations in the field, thereby obtaining more representative values for each measurement point and reducing high-frequency noise (Vargemezis et al., 2024; Widyaningrum et al., 2018).

The next step is the Fraser filtering process, which is used to smooth the data and highlight conductive anomalies in the in-phase curve. This technique was first proposed by Fraser (1969) as a simple linear filtering method to transform the intersection point pattern into a more easily interpretable peak anomaly shape. In general, the Fraser Filter equation can be expressed as (Fraser, 1969):

$$F_n = (M_{n+2} + M_{n+3}) - (M_n + M_{n+1}) \tag{1}$$

where M_n is the in-phase value at the n-th measurement point. The results of this filter are displayed as a Fraser plot, where positive and negative values reflect the possible presence of more conductive or more resistive materials beneath the measurement point, which qualitatively aids in determining the lateral position of the anomaly (Alao et al., 2024; Al-Tarazi et al., 2008; Sundararajan et al., 2006).

The next step is the Karous–Hjelt filtering process, which is used to model the distribution of apparent current density in the form of a two-dimensional vertical cross-section. This technique, developed by Karous and Hjelt (1983), is a more general form of the Fraser Filter because it is derived directly from the concept of the magnetic field associated with subsurface current flow (Desifatma et al., 2024; Gürer et al., 2009; Karous & Hjelt, 1983). The Karous–Hjelt Filter equation can be expressed as (Karous & Hjelt, 1983):

$$\begin{aligned} K = \frac{\Delta z}{2\pi} = {} & (-0.102 \times M_{n-3}) + (0.059 \times M_{n-2}) - (0.561 \times M_{n-1}) \\ & + (0.561 \times M_{n+1}) - (0.059 \times M_{n+2}) + (0.102 \times M_{n+3}) \end{aligned} \tag{2}$$

where K is the apparent current density, Δz is the spacing between measurement points (distance between stations), and M_n is the filtered magnetic field value (typically from the in-phase component). The result of this filtering process yields apparent current density values, which are then visualized in the form of graphs or two-dimensional cross-sectional models of subsurface conductivity distribution. These are subsequently used to identify zones of conductive anomalies that may be associated with geological structures such as faults, fractures, water-saturated zones, or mineralization (Al-Tarazi et al., 2008; Gürer et al., 2009; Ogilvy & Lee, 1991; Purwanto et al., 2015). The results are visualized as part of the data processing output once the entire numerical processing procedure is complete. The visualization stage displays the processed results in the form of Fraser Filter graph, Karous–Hjelt Filter graph, and two-dimensional pseudo-section contours. Additionally, the software provides options to display out-phase and field strength graphs as part of the visualization of the measurement data.

Overall, the VLF-EM data processing workflow implemented in DEXS begins with importing field measurement data, followed by averaging repeated measurements, applying the Fraser Filter and the Karous–Hjelt Filter, visualizing the processed results, and finally exporting the numerical data and visualization results. This sequence of processing steps is shown in Figure 1, which illustrates the integration of all processing stages into a single workflow within DEXS. Each stage produces an output that serves as the input for the next stage, allowing the processing sequence to proceed systematically from data import to result export. This integrated design allows the entire VLF-EM data processing procedure to be carried out within a single application without requiring additional software.

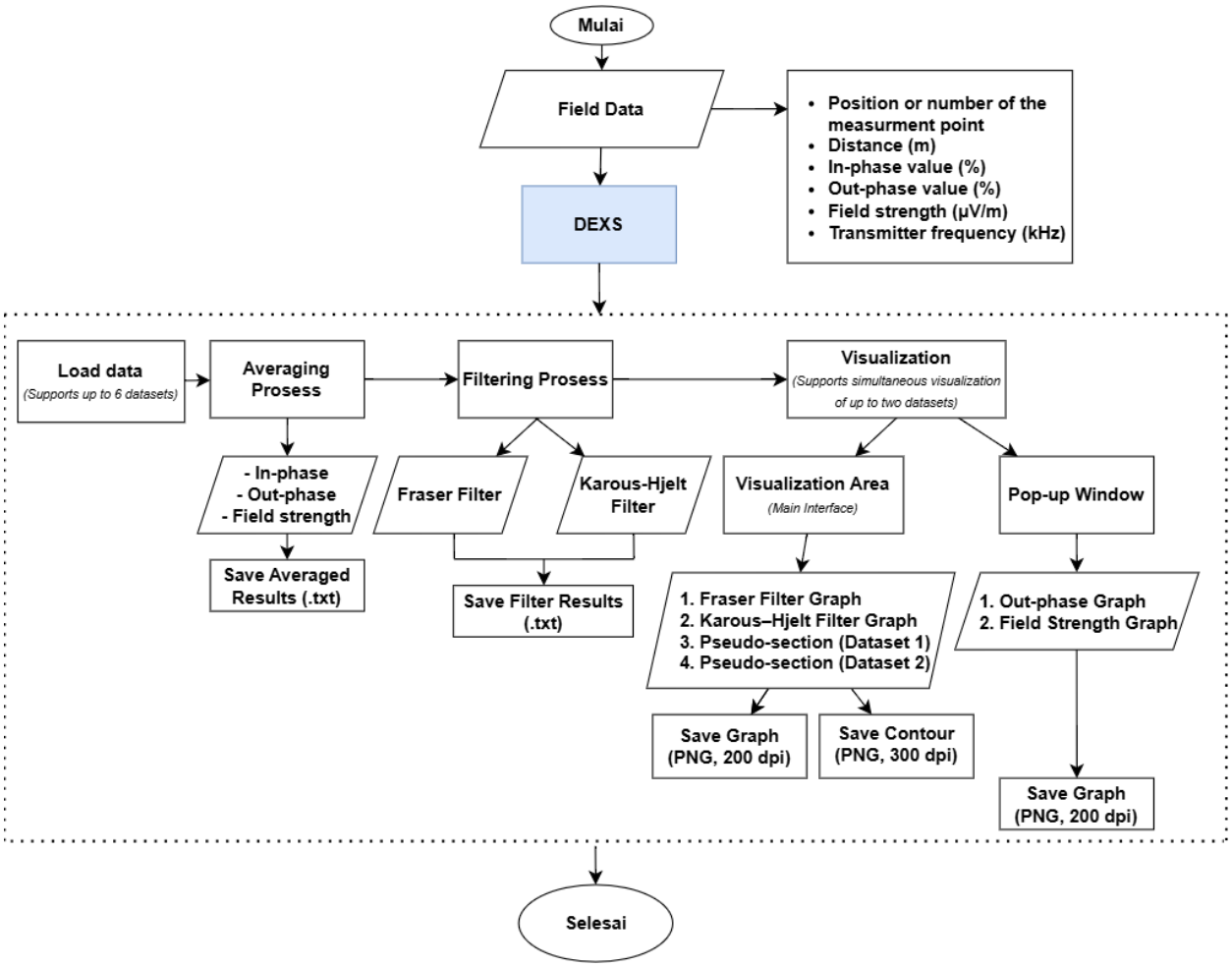


Figure 1. VLF-EM Data Processing Workflow Implemented in DEXS

2.4 DEXS Design

DEXS was designed and implemented using GNU Octave version 10.1.0 as the programming platform. The program was developed as a script with the .m extension, which serves as the main file for running the data processing system. Through this file, the software named DEXS can be activated to read data, perform processing, and visualize the results of VLF-EM data processing via a simple GUI-based graphical interface that has been designed.

The DEXS Graphical User Interface (GUI) was built using GNU Octave's built-in interface components, such as *uicontrol*, *axes*, and *callback functions*, to link each stage of data processing within a single integrated interface. This software is organized into several main modules, including data loading, calculation of the average of repeated measurements, application of the Fraser Filter, application of the Karous–Hjelt Filter, visualization of results, and data export. Each module is designed to perform a specific processing function and is interconnected via the main interface, allowing all stages of VLF-EM data processing to be performed sequentially within a single application without requiring additional software. The design flow and workflow of the DEXS software are shown in Figure 2.

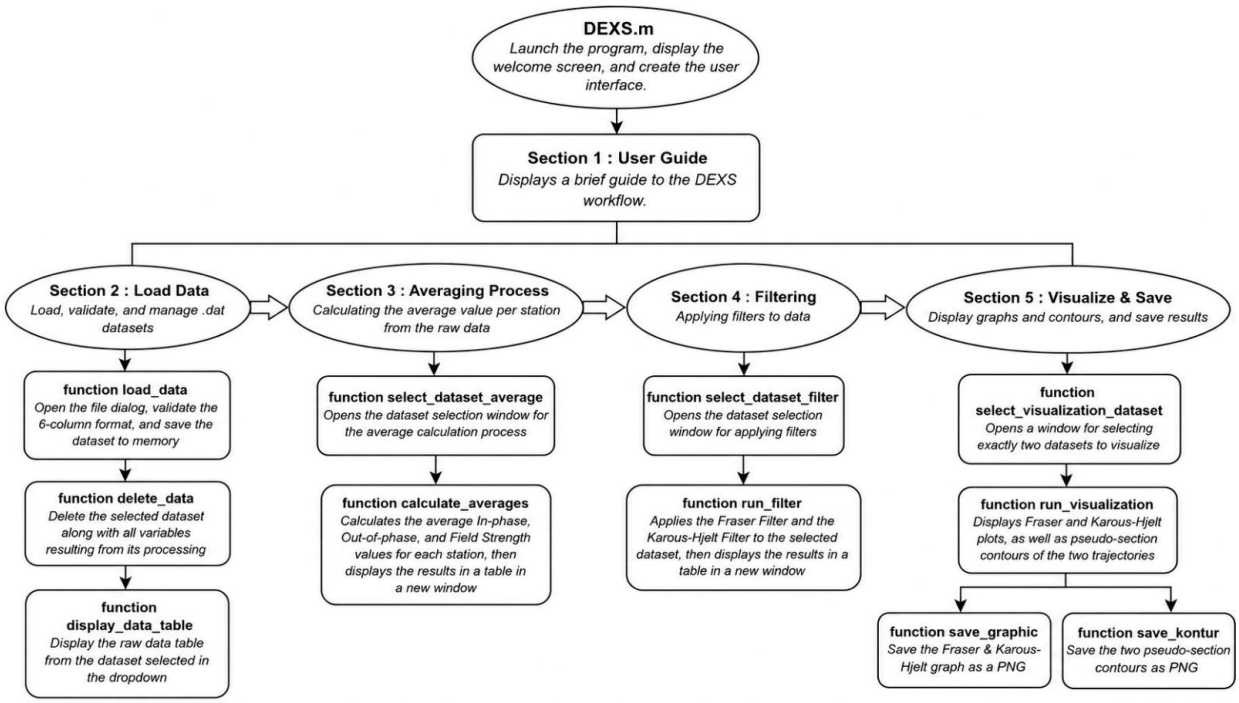


Figure 2. DEXS Design Flowchart

3. RESULT AND DISCUSSION

3.1 DEXS Graphical User Interface and Features

The DEXS software was developed as a Graphical User Interface (GUI) designed to be simple, intuitive, and ready to use without requiring any programming knowledge. Figure 3 shows the DEXS main screen, the result of a software design that integrates all major stages of VLF-EM data processing into a single interface. This approach allows data loading, processing, visualization, and result storage to be performed sequentially in a single workflow, making the processing workflow more systematic and minimizing the need for additional software. Structurally, the DEXS interface consists of three main components: the data control panel, the visualization area, and the results storage panel, each designed to support the integrated stages of data processing. The main interface of this software is shown in Figure 3.

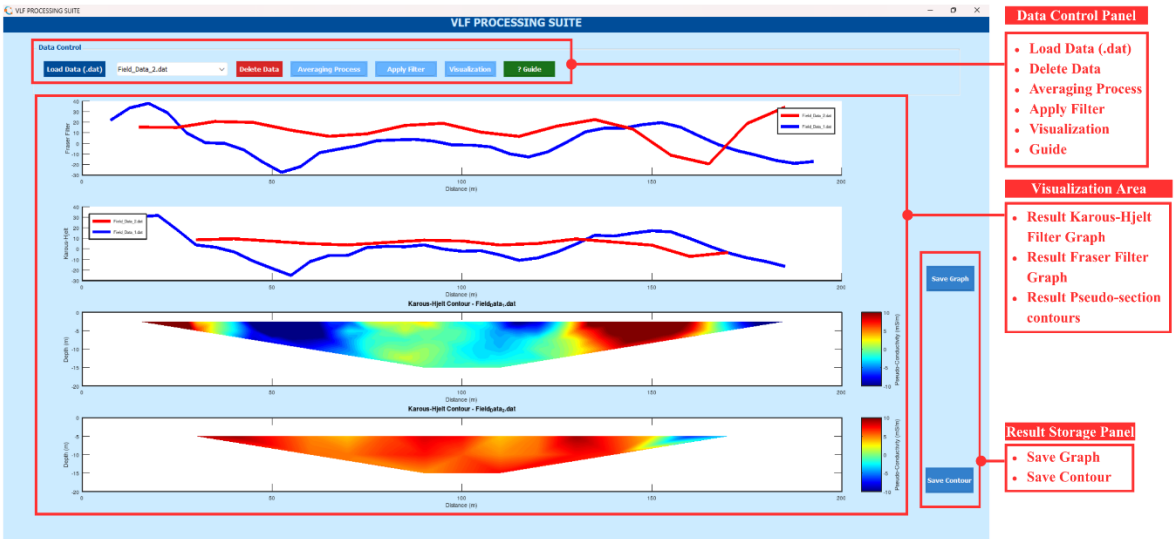


Figure 3. Main Interface of DEXS–VLF Processing Suite

The data control panel is located at the top of the application window and contains all the interactive elements used in the processing. This panel includes a Load Data (.dat) button for loading VLF-EM measurement data files in .dat format, with the capacity to load up to six datasets simultaneously in a single session. Loaded datasets are automatically listed in the dataset selector dropdown menu, which also displays the raw data table whenever the user changes their selection. Dataset management is further supported by the Delete Data button, which removes unnecessary datasets from the system. Data processing is carried out in stages using three main action buttons, Averaging Process to compute the average value from three measurements for each station along a single profile, Apply Filter to simultaneously apply the Fraser Filter and the Karous–Hjelt Filter to the selected dataset, and Visualization to display all processing results in the form of graphs and pseudo-section contours. In addition, the control panel includes Guide button that provides integrated user documentation within the application.

The visualization area is the largest component of the interface and consists of four graph panels displayed vertically. The first and second panels display the Fraser Filter and the Karous–Hjelt Filter graphs, respectively. Both graphs support the simultaneous display of two tracks, for example two different data acquisition paths within the survey area distinguished by blue for Track 1 and red for Track 2, accompanied by a legend that is adaptively positioned in the corner of the graph. The third and fourth panels display Karous–Hjelt pseudo-section contours for each track in the form of two-dimensional cross-sections. These contours are generated by interpolating the data into an 800×400-point grid, which is then smoothed with a Gaussian smoothing (sigma value of 2). This choice of sigma value was made to strike a balance between reducing interpolation artifacts and preserving the shape of the main anomalies, so that the pseudo-conductivity distribution pattern is maintained without producing contours that are either too coarse or overly smoothed (Gonzalez & Woods, 2018). Contour visualization uses a jet color scheme with a value range of −10 to +10 mS/m, where warm colors (red–brown) represent zones of high pseudo-conductivity and cool colors (blue) represent zones of low pseudo-conductivity. The horizontal axis on both contour panels represents the measurement distance in meters, while the vertical axis represents the effective depth in meters, derived from the spacing between measurement points using the Karous–Hjelt algorithm (1983).

In addition to the four graph panels displayed on the main interface, the visualization area also provides the option to display out-phase and field strength graphs via separate pop-up windows that appear independently outside the main interface. Both graphs can be optionally enabled through the visualization selection menu before the display process begins. This separation of views is intentional so that the main interface remains focused on the Fraser and Karous–Hjelt Filter results as the primary output of the processing, while the out-phase and field strength graphs are available as supplementary information that users can access as needed. Each of these graph windows also includes a Save Graph button that allows users to save the visualization results in either PNG or JPG format.

The results storage panel is located on the right side of the application window and consists of two export buttons. The Save Graph button automatically saves the Fraser Filter and Karous–Hjelt Filter graphs as two separate PNG files with a resolution of 200 dpi, while the Save Contour button saves both pseudo-section contours with a resolution of 300 dpi. In addition, each results table, whether the average table or the filter table, includes a Save as .txt button that allows numerical data to be exported in a tab-delimited structured text format, making it suitable for documentation or further analysis in other software. In general, the DEXS interface is designed to integrate all stages of VLF-EM data processing into a single, structured system, from data loading and filtering to result visualization and the export of data and graphs. This integration allows the processing to be carried out more efficiently and systematically through a GUI-based interface.

3.2 Performance Evaluation and Comparison with KHFILT

DEXS software testing was conducted by comparing the results of VLF-EM data processing with those of the KHFILT software, which has been widely used in VLF-EM data processing, particularly in the filtering and visualization stages. This testing aims to evaluate the validity and consistency of the output generated by DEXS. The data used in this testing consists of VLF-EM measurement results from the Special Region of Yogyakarta. This location was chosen because it is geologically traversed

by the X Fault system, which is one of the major active structures in Yogyakarta. The presence of this fault makes this location relevant as a test site, given that fault zones are generally more conductive than the surrounding rocks due to the presence of fractures that increase permeability and allow for the accumulation of subsurface fluids (Reynolds, 2011); thus, it is expected to be clearly recorded in the processed VLF-EM data. Data processing results for both survey lines revealed high pseudo-conductivity anomalies characterized by a predominance of red on the pseudo-section map, which were interpreted as a response to the fault zone. These conductive anomalies appear consistently at specific distances along the survey lines, indicating that the subsurface fault structures were successfully detected and visualized using both compared software packages (Figures 8 and 9).

During the testing process, the same dataset was used as input for both software programs. There are several fundamental differences in data processing capabilities between the two. In KHFILT, the average of repeated measurements must be calculated manually using external software before the data can be imported. Furthermore, KHFILT only accepts input in the form of distance columns and in-phase values, so it cannot display graphs of the out-phase component or field strength. KHFILT is also only capable of processing and visualizing one dataset per processing session. In contrast, DEXS automatically integrates all processing steps into a single interface, supports complete input of six measurement parameter columns, can visualize up to two trajectories simultaneously, and provides out-phase and field strength graphs as supplementary information. In this study, the comparison of Fraser Filter graphs and pseudo-section contours was performed directly against the output of the KHFILT software. The comparison of Karous–Hjelt graphs, however, was made against the Karous–Hjelt output values from KHFILT, which were then re-visualized as graphs using Microsoft Excel. This is because KHFILT only presents Karous–Hjelt results as numerical data, and its pseudo-section map does not provide direct graphical visualization.

A comparisons of visual and quantitative results between DEXS and reference software are shown in Figures 4 through 9, which include Karous–Hjelt plots, Fraser Filter plots, cross-plot analyses, and pseudo-section maps for the two sets of field data used. The comparison begins with the results of the Karous–Hjelt Filter graphs, as shown in Figure 4. In general, both software programs produce consistent curve patterns, with positive and negative anomalies appearing at relatively the same distances for both field datasets. The amplitude of the Karous–Hjelt values generated by DEXS falls within a range comparable to that of KHFILT. Similar consistency was also identified in the comparison of Fraser Filter graphs in Figure 5, where the patterns of anomaly peaks and troughs generated by DEXS align with the KHFILT results for both field datasets. The positions of the Fraser anomaly peaks, which reflect the presence of subsurface conductive zones, were identified at consistent distance ranges between the two software programs. This consistency indicates that the implementation of the Fraser Filter and Karous–Hjelt Filter equations in DEXS is consistent with the mathematical formulations stated in Equations (1) and (2). However, visual pattern consistency alone is not sufficient to demonstrate that the numerical values generated by the two software programs are truly equivalent. Therefore, quantitative validation was performed using cross plot analysis between the DEXS and KHFILT outputs.

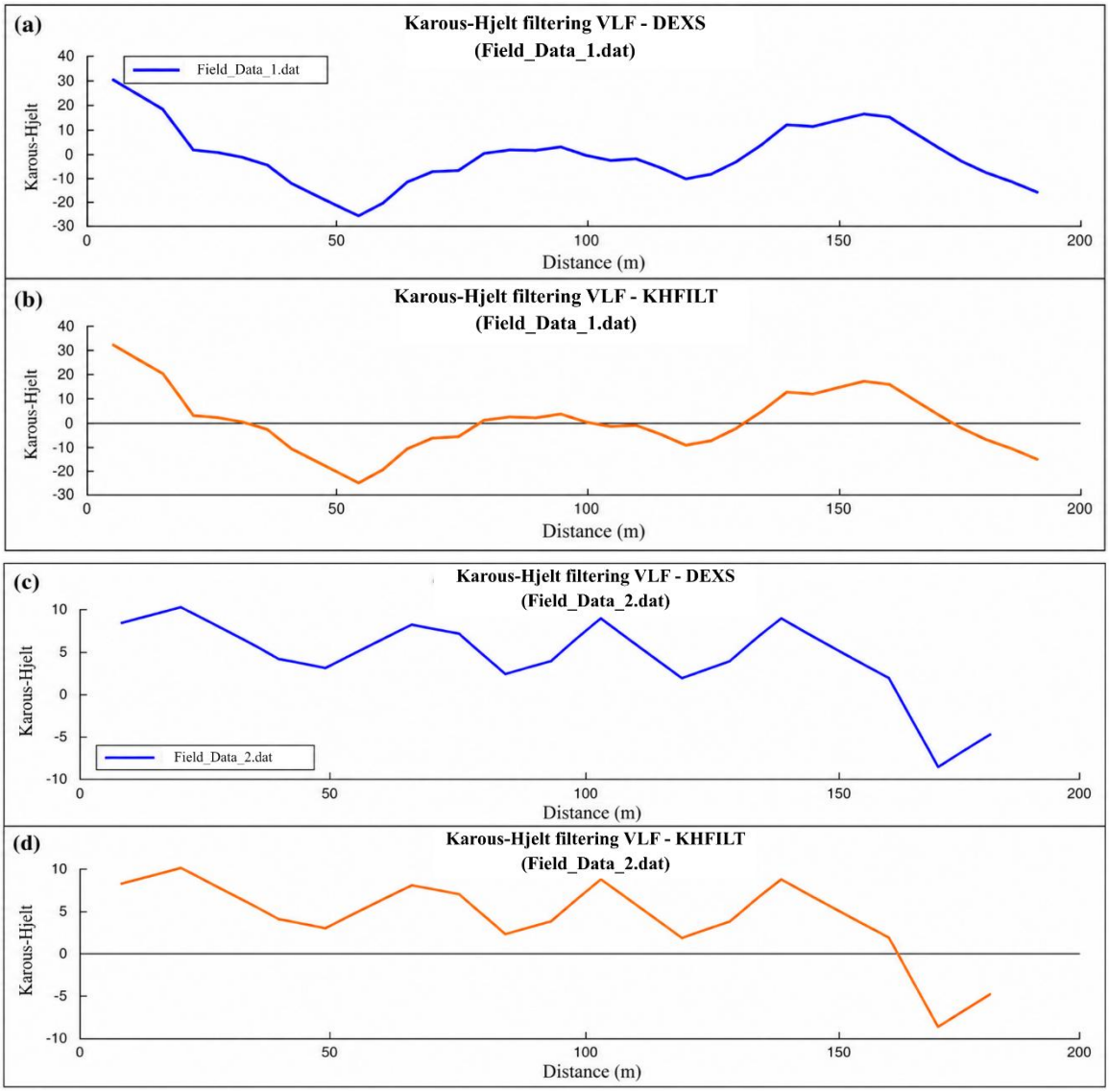


Figure 4. Comparison of Karous–Hjelt plots. (a) Plot of Field Data 1 generated by the DEXS software. (b) Plot of Field Data 1 visualized using Microsoft Excel based on the Karous–Hjelt output values from the KHFILT software. (c) Plot of Field Data 2 generated by the DEXS software. (d) Graph of Field Data 2 visualized using Microsoft Excel based on the Karous–Hjelt output values from the KHFILT software.

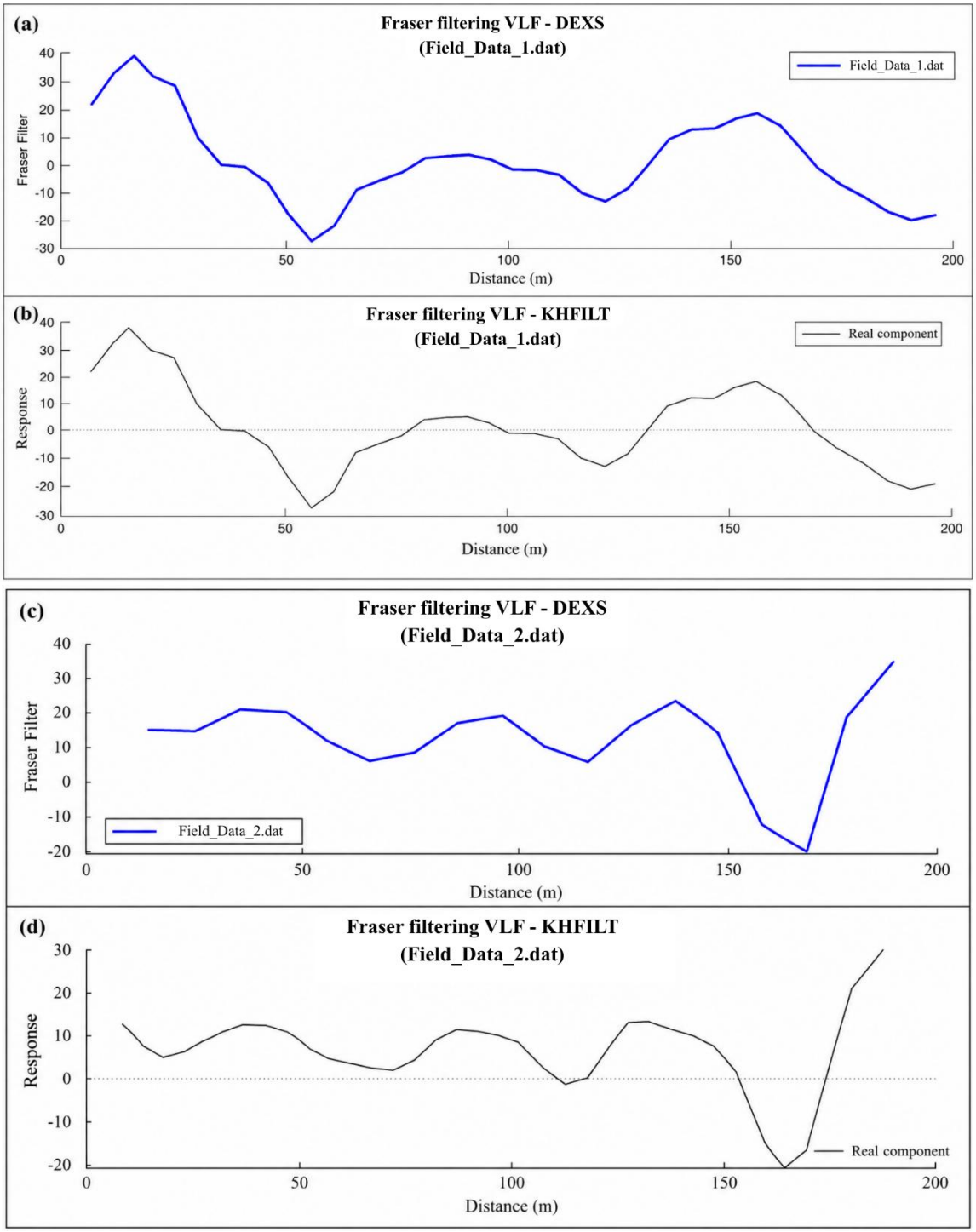


Figure 5. Comparison of Fraser plots. (a) Visualization of Field 1 data using the DEXS software. (b) Visualization of Field 1 data using the KHFILT software. (c) Plot of Field 2 data generated by the DEXS software. (d) Plot of Field 2 data generated by the KHFILT software.

The visual agreement observed in the Fraser Filter and Karous–Hjelt plots was subsequently verified through quantitative validation using linear regression analysis, as presented in Figures 6 and 7.

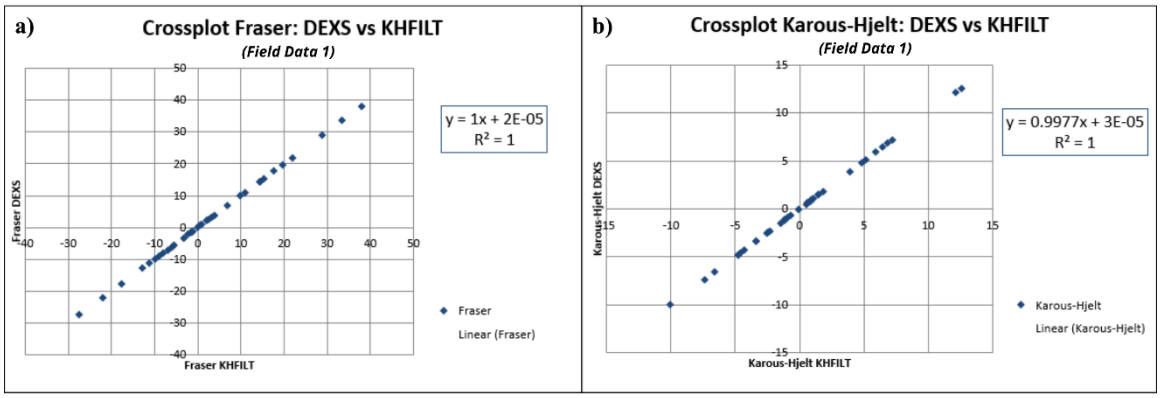


Figure 6. Cross plot of the quantitative validation results between the values generated by DEXS and the comparison software. (a) Comparison of DEXS Fraser Filter values with KHFILT for Field Data 1. (b) Comparison of DEXS Karous–Hjelt values with KHFILT for Field Data 1.

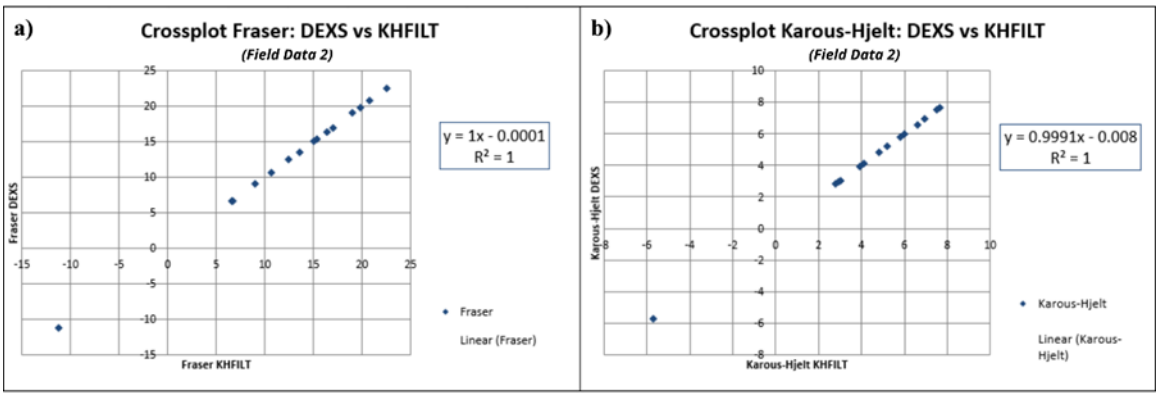


Figure 7. Cross plot of the quantitative validation results between the values generated by DEXS and the comparison software. (a) Comparison of DEXS Fraser Filter values with KHFILT for Field Data 2. (b) Comparison of DEXS Karous–Hjelt values with KHFILT for Field Data 2.

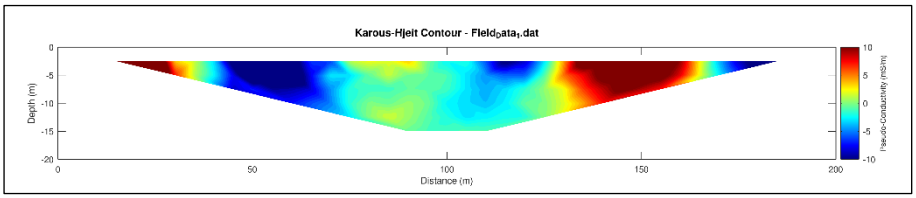
To facilitate comparison of the quantitative validation results between the two field datasets, the coefficient of determination (R^2), regression slope, and intercept obtained from the linear regression analysis are summarized in Table 1. The very small differences in the slope and intercept values are likely attributable to numerical rounding (floating-point arithmetic) during the computation process and do not significantly affect the interpretation of the results.

Table 1. Summary of Quantitative Validation Results Comparing DEXS and KHFILT

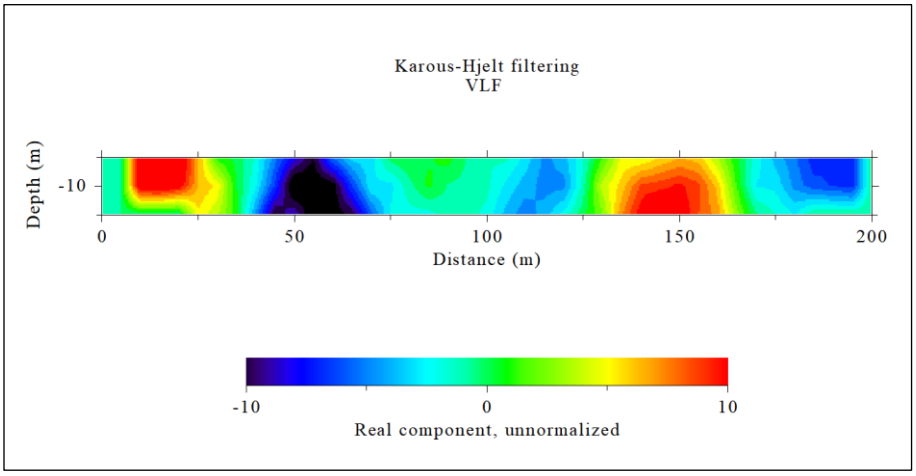
Data Set	Filter Type	Regression Equation	R^2	Slope	Intercept
Field Data 1	Fraser Filter	$y = 1x + 2 \times 10^{-5}$	1	1	2×10^{-5}
Field Data 1	Karous-Hjelt Filter	$y = 0.9977x + 3 \times 10^{-5}$	1	0.9977	3×10^{-5}
Field Data 2	Fraser Filter	$y = 1x - 0.0001$	1	1	-0.0001
Field Data 2	Karous-Hjelt Filter	$y = 0.9991x - 0.008$	1	0.9991	-0.008

Visual validation using Fraser Filter and Karous–Hjelt plots, as well as quantitative validation using cross plot analysis, showed that the filtering results produced by DEXS were consistent with those from KHFILT. The next step focused on comparing the pseudo-section visualizations generated by the two software programs. Comparisons of the pseudo-section map results for Field Data 1 and Field Data 2 are shown in Figure 8 and Figure 9, respectively. Qualitatively, the distribution of high- and low-pseudo-conductivity zones in the DEXS output shows a pattern consistent with the KHFILT results, both in terms of horizontal position and the trend of anomaly distribution with depth. High pseudo-conductivity zones, marked in red to brown with values ranging from +5 to +10 mS/m, and low pseudo-conductivity zones, marked in blue with values ranging from −5 to −10 mS/m, appear at comparable distances and depths in both software programs. In Field Data 1, the DEXS shows a varied

distribution with conductive zones (red-brown with a range of approximately +7 to +10 mS/m) on the left (0–40 m) and right (140–200 m) sides of the profile, as well as resistive zones (blue, ranging from −7 to −10 mS/m) in the central section (40–80 m), which is consistent with the KHFILT results and can be interpreted as an indication of fault structures, where the conductive zones are associated with fluid-saturated fractures and the resistive zones reflect more compact material. The consistency in spatial distribution, anomaly geometry, and apparent conductivity range between the output results of the two software programs for Field Data 1 can be seen in Figure 8.



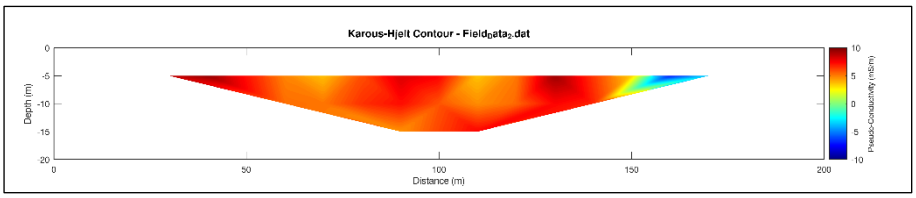
(a)



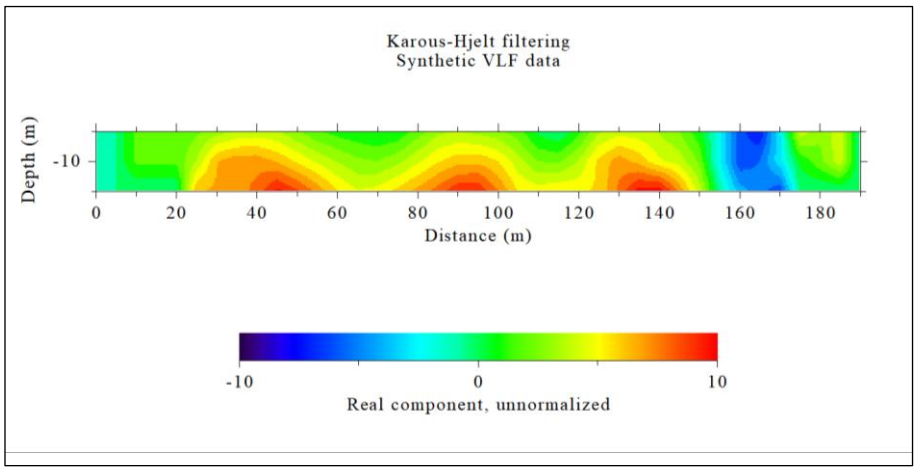
(b)

Figure 8. Comparison of pseudo-section map results. (a) Visualization of Field 1 data using the DEXS software. (b) Visualization of Field 1 data using the KHFILT software.

In contrast to Field Data 1, the pseudo-section comparison for Field Data 2, presented in Figure 9, is dominated by conductive zones across nearly the entire profile (0–160 m) at various depths, with pseudo-conductivity values ranging from +5 to +10 mS/m, while resistive zones with values around −2 to −5 mS/m appear only at the right end of the profile (155–200 m). This pattern aligns with the Karous–Hjelt plot, which shows predominantly positive values, and is consistent with the general characteristics of fault zones that have high permeability due to fractures, thereby allowing for fluid accumulation that plays a role in increasing the rock's electrical conductivity (Gürer et al., 2009; Reynolds, 2011). Meanwhile, the resistive zone at the end of the profile likely represents the lateral boundary of the influence of that fault structure, where the surrounding rocks are less fractured and therefore exhibit relatively lower electrical conductivity (Al-Tarazi et al., 2008; Ogilvy & Lee, 1991). The relatively continuous distribution of conductive zones along the profile also indicates that the recorded electromagnetic response is consistent across different pseudo-depth levels. Agreement in the positions and spatial distributions of conductive and resistive zones between the DEXS and KHFILT outputs demonstrates that both software packages produce comparable representations of subsurface anomalies. No significant shifts in the locations of the main anomalies or changes in the overall anomaly distribution pattern were observed between the two visualizations, indicating that the resulting geological interpretation remains consistent. The comparison of the pseudo-section maps for Field Data 2 generated by DEXS and KHFILT is presented in Figure 9.



(a)



(b)

Figure 9. Comparison of pseudo-section map results. (a) Visualization of Field 2 data using DEXS software. (b) Visualization of Field 2 data using KHFILT software.

The visually apparent differences between the two software programs lie primarily in the shape of the lower boundary of the cross-section and the level of smoothness of the resulting contour. In DEXS, areas outside the range of the interpolated data are not forcibly filled in but are left empty without values, resulting in a triangular lower contour boundary that follows the geometry of the available pseudo-section points. This condition is a direct consequence of the Karous–Hjelt algorithm, which constructs pseudo-sections in a hierarchical manner based on the spacing between measurement points; the greater the modeled effective depth, the fewer data points are available for the interpolation process. This approach is considered more scientifically conservative than filling empty areas with extrapolation, as it does not add information beyond the data's actual resolution. The use of extrapolation in areas without data control can produce interpolation artifacts, such in spurious anomalies or contour patterns that do not represent the actual subsurface conditions (Billings et al., 2002; Telford et al., 1990). Meanwhile, the difference in contour smoothness between DEXS and KHFILT is due to the application of Gaussian smoothing in DEXS, which aims to reduce interpolation artifacts, resulting in visually smoother contours without significantly altering the locations or overall geometry of the main anomalies (Gonzalez & Woods, 2018).

Overall, the test results show that the DEXS software is capable of producing valid and consistent output compared to the KHFILT software used as a benchmark. Visual validation reveals consistency in anomaly patterns on the Fraser Filter plot, the Karous–Hjelt plot, and the pseudo-section map, while quantitative validation via cross plot analysis confirms the previously reported strong linear agreement of $R^2 > 0.999$ between DEXS and KHFILT. In addition to the validity of the processing results, DEXS is also capable of integrating all stages of VLF-EM data processing, ranging from data loading, calculation of the average of repeated measurements per station, application of the Fraser Filter and Karous–Hjelt Filter, to exporting results in the form of graphs or numerical data, within a single integrated interface that can be fully operated via button-based interactions without requiring any programming knowledge. Thus, users can perform the entire VLF-EM data processing workflow comprehensively and systematically using just a single .m script file to run on the GNU Octave platform. This makes DEXS a freely accessible alternative to geophysical data processing software without licensing restrictions, giving it the potential for widespread use in academic

settings, particularly by students who need a practical and affordable tool for VLF-EM data processing.

The development of DEXS also contributes to physics education by providing an open-source platform for learning VLF-EM data processing, particularly in the areas of earth physics, electromagnetic methods, and scientific computing. The integration of all data processing stages into a single interface allows students to understand the data processing workflow systematically, while also providing an easily accessible alternative for educational institutions with limited access to commercially licensed software. Thus, DEXS has the potential to be utilized as a learning medium, a tool for data processing labs, and a training tool to support student learning and research activities in the field of earth physics.

4. CONCLUSION

This study demonstrates that DEXS was successfully developed with a Graphical User Interface (GUI) on the GNU Octave platform as an open-source alternative for VLF-EM data processing, free from licensing constraints. DEXS is capable of integrating all stages of data processing in a unified manner, ranging from data loading, calculation of the average of repeated measurements per station, application of the Fraser Filter and Karous–Hjelt Filter, to the visualization of results in the form of graphs and two-dimensional pseudo-section maps, thereby facilitating analysis for users. Test results using two field datasets show that the output generated by DEXS exhibits excellent agreement with the KHFILT software, both for the Fraser Filter and the Karous–Hjelt Filter results. This consistency is demonstrated by a consistent pattern of anomalies and confirmed by cross plot analysis. A coefficient of determination $R^2 > 0.999$, a regression slope approaching one, and an intercept approaching zero indicate that DEXS is valid for use in the qualitative interpretation of subsurface structures. In addition, DEXS also has advantages over KHFILT, namely support for six-column measurement parameter input, the ability to display two trajectories simultaneously, and the provision of out-phase and field strength graphs as additional information.

For further development, it is recommended that DEXS enhance its visualization capabilities to display more than two trajectory datasets in a single interface, thereby enabling a more comprehensive comparative analysis of trajectories. Furthermore, the addition of a spatial mapping feature is also necessary so that users can plot the coordinates of each measurement station, thereby visualizing the direction and position of the traces more clearly and facilitating the process of correlating traces.

ACKNOWLEDGEMENTS

The author would like to thank the Department of Geophysics, Faculty of Mathematics and Natural Sciences, Padjadjaran University, for the facilities and resources provided during the course of this research.

REFERENCES

Alao, J. O., Lawal, K. M., Dewu, B. B. M., & Raimi, J. (2024). Estimation of top depth to underground targets of Karous-Hjelt and Fraser filtering of VLF-EM measurements: The Thumb's rule approach. *Geosystems and Geoenvironment*, *3*(4). https://doi.org/10.1016/j.geogeo.2024.100319

Al-Tarazi, E., Abu Rajab, J., Al-Naqa, A., & El-Waheidi, M. (2008). Detecting leachate plumes and groundwater pollution at Ruseifa municipal landfill utilizing VLF-EM method. *Journal of Applied Geophysics*, *65*(3–4), 121–131. https://doi.org/10.1016/j.jappgeo.2008.06.005

Billings, S., Beatson, R., & Newsam, G. (2002). Interpolation of geophysical data by continuous global surfaces. *Geophysics*, *67*(6), 1810–1822. https://doi.org/10.1190/1.1527081

Desifatma, E., Pratomo, P. M., Mustopa, E. J., & Srigutomo, W. (2024). VLF-EM data conversion into apparent resistivity using the Hilbert transform and its application for shallow fault investigation at Pinggirsari, Bandung Regency, Indonesia. *Heliyon*, *10*(9). https://doi.org/10.1016/j.heliyon.2024.e30878

Fraser, D. C. (1969). Contouring of VLF-EM data. *Geophysics*, *34*(6), 958–967. https://doi.org/10.1190/1.1440065

Gonzalez, R. C ., & Woods, R. E. . (2018). *Digital image processing*. Pearson.

Gordon, R., & Santos, F. M. (2016). *The Rebirth of VLF Geophysical Technology A new tool for cost effective imaging of the subsurface*. https://www.gemsys.ca/wp-content/uploads/2016/03/Gem_Rebirth-of-the-VLF-method_Rgordon_sageep_2016fin.pdf

Gürer, A., Bayrak, M., & Gürer, Ö. F. (2009). A VLF survey using current gathering phenomena for tracing buried faults of Fethiye-Burdur Fault Zone, Turkey. *Journal of Applied Geophysics*, *68*(3), 437–447. https://doi.org/10.1016/j.jappgeo.2009.03.011

Hutchinson, P. J., & Barta, L. S. (2002). VLF surveying to delineate longwall mine-induced fractures. *The Leading Edge*, *21*(5), 491–493. https://doi.org/10.1190/1.1481250

Jeng, Y., Lin, M. J., & Chen, C. S. (2004). A very low frequency-electromagnetic study of the geo-environmental hazardous areas in Taiwan. *Environmental Geology*, *46*(6–7), 784–795. https://doi.org/10.1007/s00254-004-1071-7

Karous, M., & Hjelt, S. E. (1983). Linear filtering of VLF dip-angle measurements. *Geophysical Prospecting*, *31*(5), 782–794. https://doi.org/10.1111/j.1365-2478.1983.tb01085.x

Khalil, M. A., & Santos, F. M. (2014). On the depth to anomaly estimation using Karous and Hjelt filter in VLF-EM data. *Arabian Journal of Geosciences*, *7*(10), 4355–4359. https://doi.org/10.1007/s12517-013-1110-3

Monteiro Santos, F. A., Mateus, A., Figueiras, J., & Gonçalves, M. A. (2006). Mapping groundwater contamination around a landfill facility using the VLF-EM method - A case study. *Journal of Applied Geophysics*, *60*(2), 115–125. https://doi.org/10.1016/j.jappgeo.2006.01.002

Ogilvy, R. D., & Lee, A. C. (1991). Interpretation of VLF-EM in-phase data using current density pseudosections. *Geophysical Prospecting*, *39*(4), 567–580. https://doi.org/10.1111/j.1365-2478.1991.tb00328.x

Paál, G. (1965). Ore prospecting based on VLF-radio signals. *Geoexploration*, *3*(3), 139–147. https://doi.org/10.1016/0016-7142(65)90016-5

Pirttijärvi, M. (2004). Manual of the KHFILT Program: Karous-Hjelt and Fraser filtering of VLF measurements (Version 1.1a). *University of Oulu, Finland*.

Purnama, A. Y., Nurhanafi, K., & Wibowo, N. B. (2025). Visualization of Microseismic Processing by Coding with GNU Octave. *Navigation Physics: Journal of Physics Education*, *7*(1).

Purwanto, E. H., Minarto, E., & Bahri, A. S. (2015). Aplikasi Metode Very Low Frequency Electromagnetic (VLF-EM) untuk Karakteristik Bawah Permukaan di Daerah Kapur Desa Melirang Kecamatan Bungah Kabupaten Gresik. *Jurnal Fisika Indonesia*, *19*(55), 38–41. https://doi.org/10.22146/jfi.24357

Quarteroni, A., Saleri, F., & Gervasio, P. (2010). *Scientific Computing with MATLAB and Octave* (Vol. 2). Springer Berlin Heidelberg. https://doi.org/10.1007/978-3-642-12430-3

Reynolds, J. M. (2011). An Introduction to Applied and Environmental Geophysics. *Preview*, *2011*(155), 33–40. https://doi.org/10.1071/PVv2011n155other

Saydam, A. S. (1981). Very low-frequency electromagnetic interpretation using tilt angle and ellipticity measurements. *Geophysics*, *46*(11), 1594–1605. https://doi.org/10.1190/1.1441166

Sundararajan, N., Ramesh Babu, V., Shiva Prasad, N., & Srinivas, Y. (2006). VLFPROS-A Matlab code for processing of VLF-EM data. *Computers and Geosciences*, *32*(10), 1806–1813. https://doi.org/10.1016/j.cageo.2006.02.021

Telford, W. M., Geldart, L. P., & Sheriff, R. E. (1990). *Applied Geophysics*. Cambridge University Press. https://doi.org/10.1017/CBO9781139167932

Vargemezis, G. N., Zlotnicki, J., Hauge, B. G., Kjøniksen, A. L., & Strand, E. P. (2024). Contribution of VLF electromagnetic survey to the investigation of Hessdalen lights (Norway). *Journal of Applied Geophysics*, *226*. https://doi.org/10.1016/j.jappgeo.2024.105398

Widyaningrum, Y., Huda, A. M., & Sungkono. (2018). Aplikasi filter EEMD untuk meningkatkan kualitas data VLF-EM: Studi kasus estimasi lokasi gorong-gorong di Kampus ITS Surabaya. *Jurnal Geosaintek, 4*(3), 125–132. https://doi.org/10.12962/j25023659.v4i3

Yadi, K., Warnana, D. D., Pandu, J., Sutra, N., & Soemitro, R. A. A. (2017). Interpretasi Filter Fraser dan Karous-Hjelt Pada Data VLF-EM Untuk Mengidentifikasi Air Lindi di Area TPA Ngipik. *Jurnal Teknik ITS*, *6*(2). https://doi.org/10.12962/j23373539.v6i2.24356

Zlotnicki, J., Le Mouël, J. L., Kanwar, R., Yvetot, P., Vargemezis, G., Menny, P., & Fauquet, F. (2006). Ground-based electromagnetic studies combined with remote sensing based on Demeter mission: A way to monitor active faults and volcanoes. *Planetary and Space Science*, *54*(5), 541–557. https://doi.org/10.1016/j.pss.2005.10.022